MECHANICAL PROPERTIES OF TITANIUM METAL MATRIX NANOCOMPOSITES REINFORCED WITH MULTIWALLED CARBON NANOTUBES, GRAPHENE AND NANODIAMONDS PREPARED BY SPARK PLASMA SINTERING

Suli Liu, Faming Zhang*,Tengfei Liu, Peipei Zhao

Jiangsu Key Lab for Advanced Metallic Materials, School of Materials Science and Engineering, Southeast University, 211189 Nanjing, China, fmzhang@seu.edu.cn.

Key words: TiMMCs, Nanocarbon, Spark plasma sintering, Mechanical properties

ABSTRACT

The nanocarbon materials including multiwalled carbon nanotubes (MWCNTs), graphene (Gr) and nanodiamonds (NDs) were used as reinforcements in the titanium metal matrix composites (TiMMCs) fabricated via ball milling and spark plasma sintering techniques. The microstructure and mechanical properties of these nanocomposites were studied by X-ray diffraction, scanning electron microscopy, transmission electron microscopy, microhardness, nanoindentation and compressive tests. Experimental results show that the Ti-0.5wt% MWCNTs composites have the best mechanical properties in the three kinds of TiMMCs. The micro-hardness and 0.2% yield strength ($\sigma_{0.2}$) of Ti-0.5wt% MWCNTs composites were 28.6% and 14.31% higher than those of the pure Ti, respectively. They showed the highest ultimate compressive strength (σ_{bc}: 2193 MPa) with ultimate strain (ε) of 62.95%. The mechanical properties of Ti-0.5wt% NDs composite were in the middle of the three kinds of TiMMCs. The Gr was not beneficial for a good interface bonding with the Ti matrix, which deteriorated their mechanical properties.

1 INTRODUCTION

Titanium (Ti) and its alloys have been found extensively applications in many engineering industries such as aerospace, chemical, and biomedical industry due to their light weight, high specific strength, good chemical resistance and excellent bio-compatibility [1-3]. However, Ti metal typically exhibits poor surface hardness, insufficient abrasive wear resistance and inadequate oxidation resistance. Ti alloys doping with elements of aluminum, vanadium, zirconium, nickel and so on have been studied [4-6]. It indicated that the mechanical properties of the Ti alloy have been increased, while the problem of release of metal irons can induce toxic effect on the healthy cells and then lead to the pain of wounds. As a result, the application of Ti and its alloys as hip and knee prosthesis are limited [7].

Ti metal matrix composites (TiMMCs), including those with powdered reinforcing particles, can be regarded as one of the most promising materials [8]. Especially, nanostructured reinforcements can offer both superior mechanical properties and reduced weight. As the new nanostructured reinforcements, multiwalled carbon nanotubes (CNTs), graphene (Gr) and nanodiamonds (NDs), all make contribution to the development of new materials with outstanding mechanical properties due to their high modulus, excellent strength and nanostructures [9-11]. Several literatures showed significant achievements in aluminum, titanium and copper matrix reinforced with CNTs [12-14]. The researchers have demonstrated the strength of pure Ti and its alloys can be effectively enhanced with weight fraction of CNTs in range from 1.5 to 15 wt% [15, 16]. In the same way, several works presented aluminum, copper, magnesium matrix composites reinforced with Gr. Many researches have discovered that Gr provided remarkable improvements in mechanical properties as for tensile strength and wear resistance [17, 18]. As another promising carbon nanostructured material, NDs have excellent mechanical and optical properties, high surface areas [19]. At present, in terms of hardness and yield strength, it has been reported to be an excellent strengthening additive for MMCs [20]. Li et al fabricated the TiMMCs reinforced with CNTs and graphite via SPS and hot extrusion, and researched the enhancement of two kinds of nanostructure carbon [12]. However, the toxicity and biocompatibility of CNTs and Gr have been widely investigated, as a consequence, the literature data concerned the biological properties and cytotoxicity of CNTs and Gr [21, 22]. NDs are non-toxic comparing to CNTs and Gr, which makes them be better suitable for biomedical application [13]. While few literature indicate that TiMMCs reinforced with NDs, and no literature present different enhancement effect of MMCs with the three kinds of nanocarbon materials.

In this work, spark plasma sintering (SPS) technique was incorporated to fabricated Ti matrix composites reinforced by uniformly dispersed nanocarbons including the MWCNTs, Gr and NDs. The effects of different kinds of nanocarbon reinforcements on the microstructure and mechanical properties of TiMMCs was investigated. A comparison study on their microstructures and mechanical properties was performed. The strengthening mechanisms using of CNTs, Gr and NDs in the Ti matrix were discussed.

2 EXPERIMENTAL PROCEDURE

2.1 Starting materials

The Ti powders with a purity of 99.5% and average particle size of 325 mesh were obtained from Nanjing Mingshan Advanced Materials Co. Ltd, China. MWCNTs with diameter of 10-40 nm, length >5 μm and purity of 98% were offered by Shenzhen Nanotech Port Co. Ltd., China. Single layer Gr with purity of 99% was supplied by ASC Material, LLC., USA. NDs with a purity of >98% and about 5 nm diameter was purchased from Tianjin with Chanyu Superhard Sci-Tech Co. Ltd. China.

2.2 Preparation of the nanocomposite

Appropriate MWCNTs, Gr and NDs reinforcements of 0.25 and 0.5 wt.% were mixed with the Ti powders, respectively. In order to achieve an optimal distribution of reinforcement in the Ti matrix powders, they were mixed via a two-stage process as shown in Figure 1. In stage (a), the first task was used to disperse the original powders using ultrasonication in ethanol and tip sonication, respectively. Then the two liquids were mixed by the sonication. As following 5 hours wet milling was done in a high energy planetary ball milling machine (QM-3SP2) with ball to powder ratio of 10:1 at 250 RPM. The mixed powders were dried and loaded into a cylindrical graphite die (Φ10 mm), sintered via a spark plasma sintering system (SPS, FCT-HP-D5, FCT Systeme GmbH, Germany) installed at Southeast University (see stage b), The sintering parameters was set as 900 °C (holding time 10 min) which was measured by a thermocouple (TC), and at a pressure of 60 MPa in vacuum. Ultimately the samples with diameter of 10.0 mm and height of 12.0 mm were obtained.

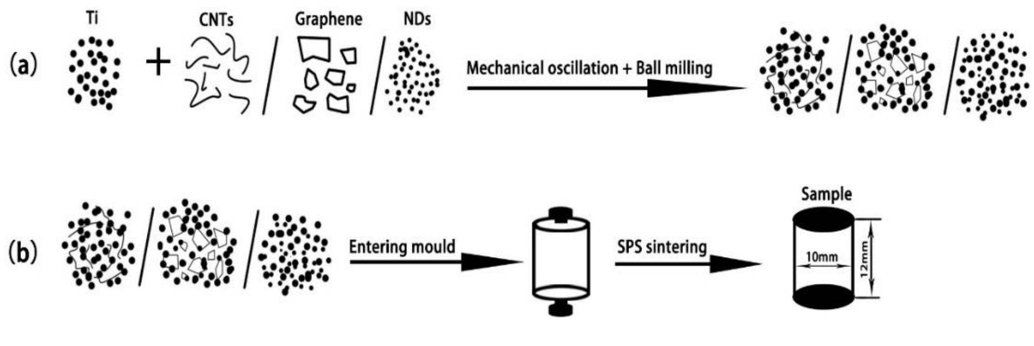

Figure 1: Schematic illustration of processing procedure for the Ti-MWCNTs/Gr/NDs nanocomposites.

2.3 Characterization

The apparent densities of all the sintered nanocomposite samples were determined at room temperature using Archimedes principle, and the the relative density relating to pure Ti matrix were calculated. The phase compositions were identified by X-ray diffraction system (XRD, D8 discover, Bruker) with Cu kα radiation. The microstructure of the samples were investigated using field-emission scanning electronic microscopy (FESEM, Sirion, FEI) and transmission electron microscopy (TEM, Tecnai, FEI). The microhardness tester (FM-700, Future-Tech Co., Tokyo) loading 3N was conducted using with a Line Set A tester mode to measure the Vickers micro-hardness. Nanoindentation test system (Micro Materials-NanoTest) equipped with a calibrated diamond Berkovich indenter tip was used to measure the Young's modulus (E). The loading parameters was set as a maximum load of 5 mN holding 5s with a loading rate of 0.25 mN/s. Compression tests were conducted on the CMT5305 testing machine (MTS Industrial Systems) loading 300 kN with a strain rate of 0.5 mm/min.

3. RESULTS AND DISCUSSION

3.1 Morphologies of the raw powders

The SEM micrograph of the Ti powders and the TEM images of the nanocarbons are shown in Figure 2. Figure 2(a) shows the SEM micrograph of pure Ti powders. The Ti powders exhibit irregular bulk shape, with mean particle sizes of 44 μm. The TEM microstructures of the MWCNTs/Gr/NDs are shown in Figure 2(b-d). It can be seen MWCNTs with diameter of 10-40 nm, single layer Gr and round nanometer sized NDs particles with a uniform particle size of 5 nm.

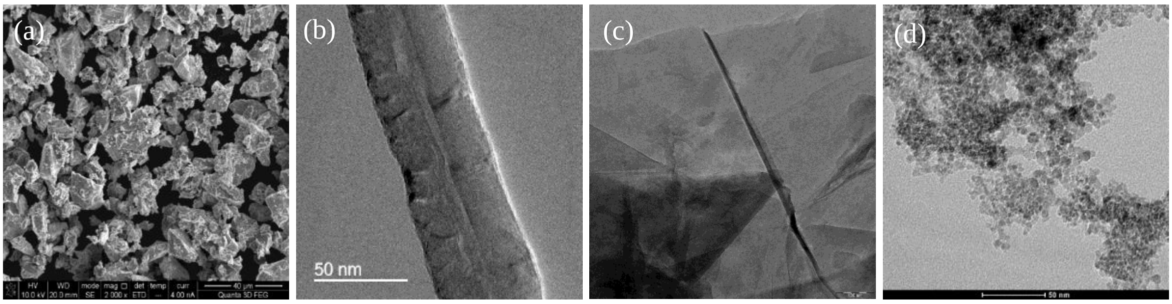

Figure 2: SEM micrograph of the pure Ti powders (a), TEM micrographs of the MWCNTs (b), Gr (c) and NDs (d)

3.2 Distribution of nanocarbons and composite density

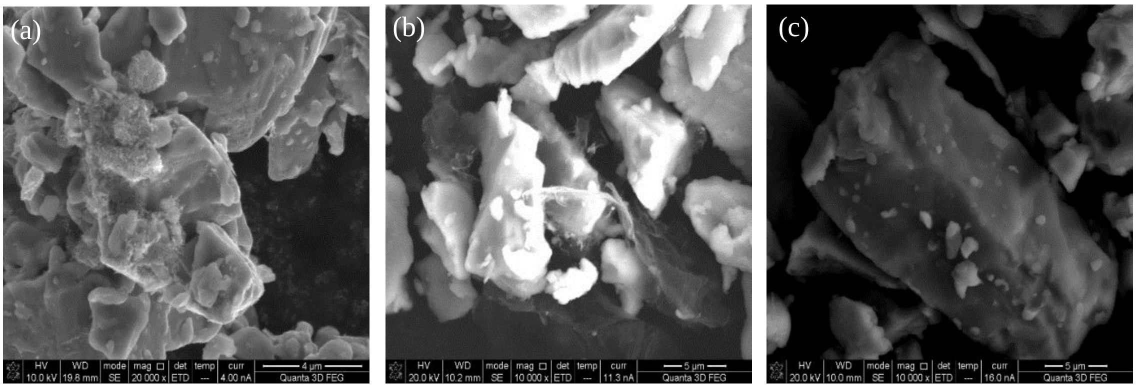

Figure 3: SEM micrographs of the powder mixtures of Ti-0.5wt% MWCNTs (a), Ti-0.5wt% Gr (b) and Ti-0.5wt% NDs (c).

Figure 3 exhibits the SEM micrographs of the morphologies of mixed powders (Ti-0.5 wt% MWCNTs/Gr/NDs). The tubular structures of the MWCNTs, sheets of the single-layer Gr and nearly spherical NDs particles are uniformly dispersed in the Ti matrix. There are a few agglomerations in the powder mixtures. It is due to their features of nano-reinforcements, like nanoscale size, large specific surface area and high surface energy, they often exhibit significant agglomerations and this feature is not easy to lose [19].

The relationship between different reinforcements and relative density of the nanocomposites are shown in Figure 4. It can be seen that the relative densities of the nanocomposites are all exceed 99%. It revealed that the SPS process can fabricated dense TiMMCs at lower temperatures. In addition, the TiMMCs with 0.5wt.% MWCNTs/NDs present relative densities up to 99.7%. The Ti-0.5wt.% Gr composite has the lowest relative density of 99.4%. Maybe it is because of the layer structured Gr is not easy to bind with the Ti matrix leading to a relative lower density.

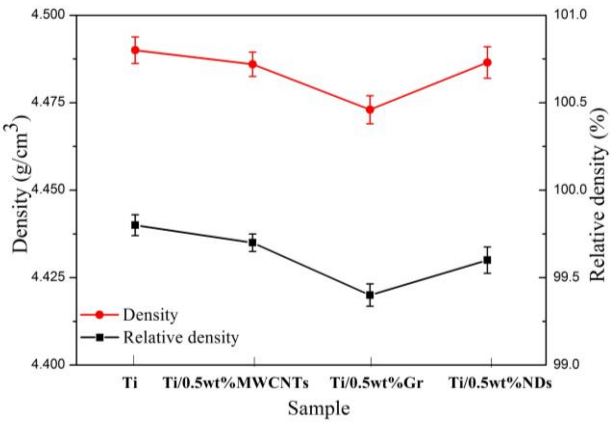

Figure 4: Density and relative density of the pure Ti, Ti-0.5 wt% MWCNTs, Ti-0.5 wt.% Gr and Ti-0.5 wt.% NDs nanocomposites.

3.3 Mechanical properties

Figure 5(a) presents the Vickers micro-hardness and the Young's modulus of pure Ti and the TiMMCs. The curves indicate that the microhardness and Young's modulus of the composites are all remarkably increased as doping of the three kinds of nanocarbons with 0.5 wt.%. The microhardness of the Ti-0.5wt% MWCNTs composites is the highest, which is 28.6% higher when compared with the value of the pure Ti. Additionally, the micro-hardness of the Ti-0.5wt% NDs composite also goes up to 339 MPa, and shows just 4.72% lower than that of the Ti-0.5wt% MWCNTs composite. An increase in hardness leads to an improvement in wear and scratch resistance of Ti matrix; this contributes to promoting the application of pure Ti and its alloys in orthopaedic implants [15]. Comparing to the microhardness, the Young's modulus of the composites are all higher than that of the pure Ti.

Room temperature compressive tests were carried out to access the stress-strain curves for the TiMMCs (Figure 5b). The compressive strength (σ_{bc}), 0.2% yield strength ($\sigma_{0.2}$) and ultimate strain (ε) measured depending on the curve of the samples are illustrated in Figure 5(c). It can be seen obviously that 0.2% yield strength ($\sigma_{0.2}$) are all much higher than that of the pure Ti. For the case of sample Ti-0.5wt% Gr, it is 14.31% higher than that of pure Ti. On the other hand, as for ultimate compressive strength (σ_{bc}), the value of Ti-0.5wt% MWCNTs composite (σ_{bc}: 2193MPa) is the highest among the three groups of TiMMCs. However the ultimate strain (ε) of the composite decreases from 62.95% (MWCNTs) to 33.89% (GR) at present study. The mechanical properties of the Ti-0.5 wt% NDs are in the middle of the three different nanocarbon reinforcements. Namely, reinforcement additive can improve the mechanical strength of the Ti abut at expense of ductility, which is consistent with the result reported by Li et al. [12].

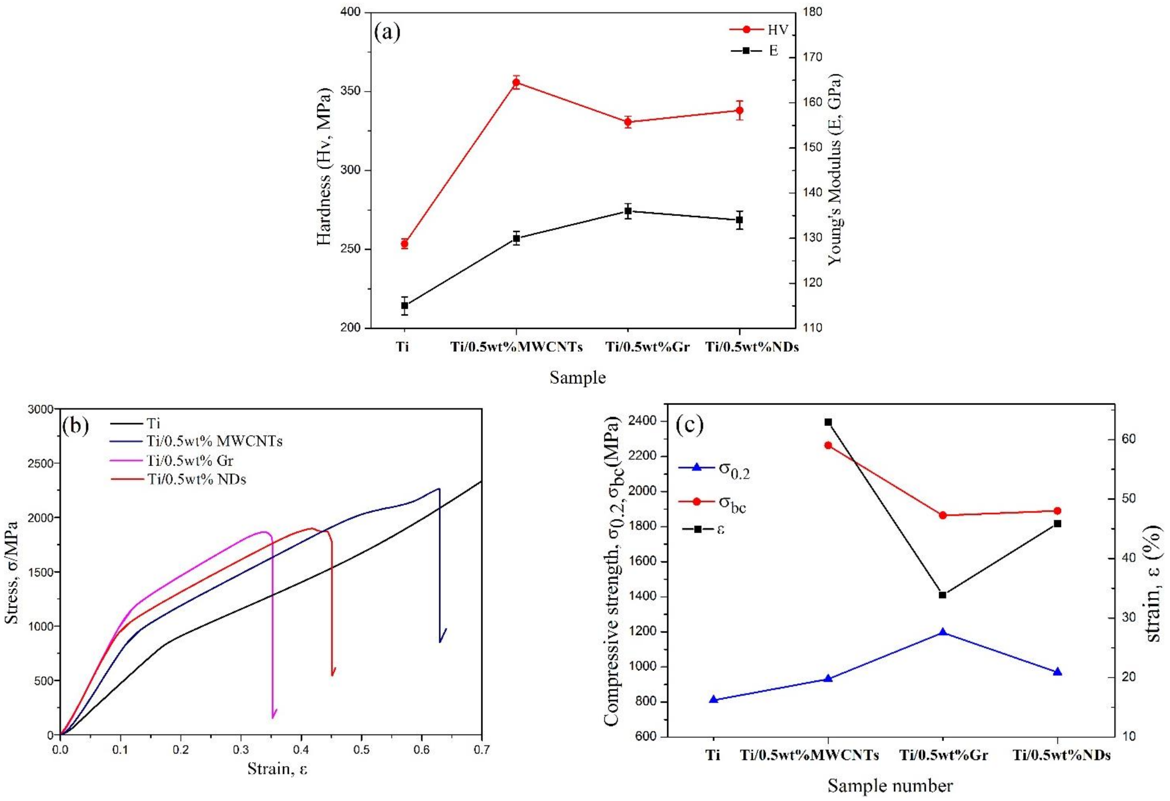

Figure 5: Mechanical properties of Ti and Ti-MWCNTs/Gr/NDs nanocomposites: hardness and Young's modulus (a), compressive stress-strain curves (b), compressive stress and strain (c) of the Ti- MWCNTs /Gr/NDs.

3.5 Microstructures

XRD spectra of the pure Ti and the TiMMCs reinforced via MWCNTs/Gr/NDs are shown in Figure 6. As can be seen, both of Ti and TiC peaks can be observed in the XRD patterns with the Ti-0.5wt% Gr/NDs composites obviously. The presence of TiC phase is confirmed by the peaks in the diffraction profile at 36.15° and 42.02° corresponding to the (111), (200) planes of TiC. The Ti-0.5wt% MWCNTs composites just show pure Ti peaks and a very weak TiC peak indexed as TiC (111). The reason is due to the NDs have many open C bonds are very active to react with the Ti matrix.

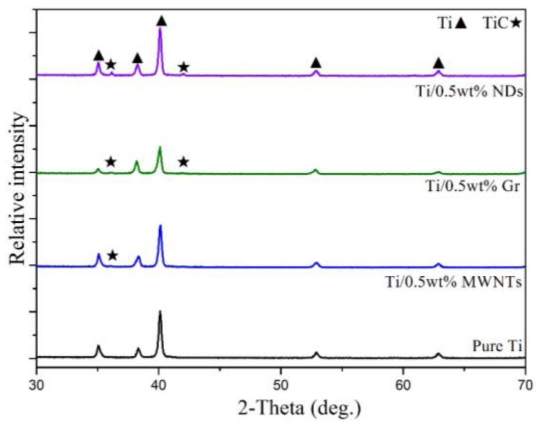

Figure 6: XRD patterns of the pure Ti and Ti-MWCNTs/Gr/NDs nanocomposites fabricated via SPS.

The fracture surfaces of the Ti-0.5wt% MWCNTs/Gr/NDs composites are presented in Figure 7. Obviously ductile dimples in the fracture surfaces can be observed as shown in the Figure 7(a). In the other TiMMCs specimen (see Figure 7b-d), they clearly show less dimples in the fractured surfaces, which indicating the composites have reduced ductility. It can be seen the presence of un-reacted MWCNTs and NDs in fracture surfaces (Figure 7b, d). And a piece of un-reacted single-layered Gr is found in the Figure 7(c). In addition, TiC particles are formed in the Ti-0.5wt% Gr/NDs composites and can be observed in the voids resulted from hard particle pull-out during the compressive tests.

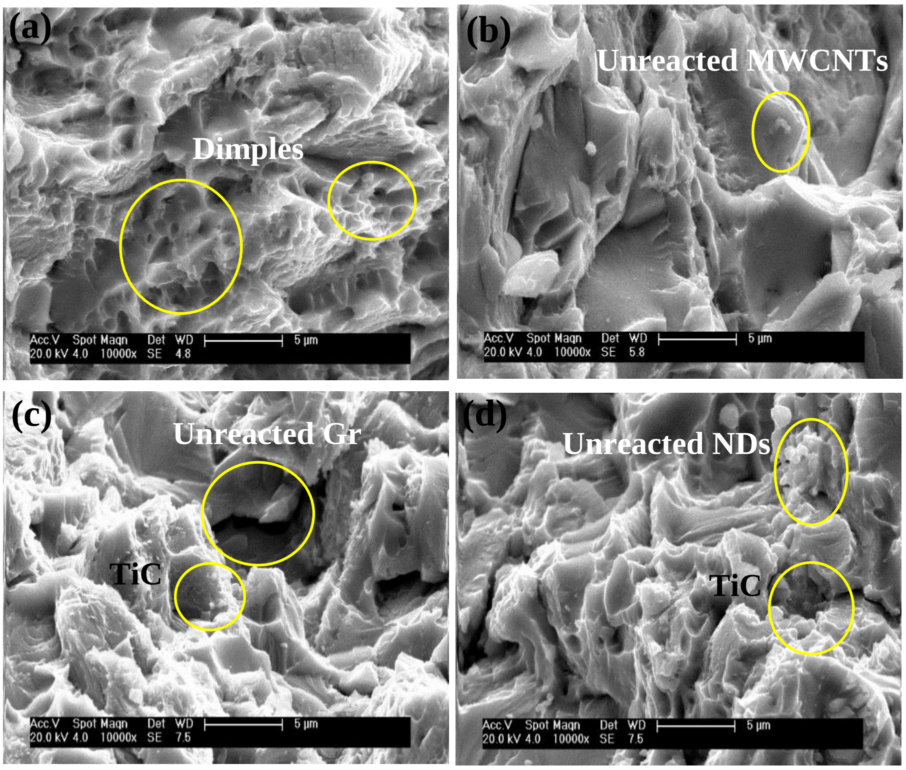

Figure 7: SEM micrographs of the fractured surfaces of pure Ti (a), Ti-0.5 wt.% MWCNTs (b), Ti-0.5 wt.% Gr (c), Ti-0.5 wt.% NDs (d)

Figure 8 exhibits the microstructures of Ti-MWCNTs/Gr/NDs composites investigated by the TEM and selected-area diffraction (SAD) patterns. The TEM images of the Ti-0.5wt% MWCNTs/Gr/NDs composites display their featured morphologies and uniformly distribution of the nanocarbon as shown in Figure 8(a-c). The three different nanometered reinforcements can be recognized from their surface morphologies. The SAD pattern of the Ti-0.5wt% MWCNTs composites as inserted in Figure 8(a) is investigated. The (111) and (220) planes of carbon are matched with the MWCNTs. In the image of the Ti-0.5wt% Gr composite (Figure 8b), several single-layer Gr can be observed. The SAD pattern inserted in Figure 8(b) shows that the measured lattice fringes of 0.203 and 0.123 nm are corresponding to the (110) and (101) planes of Gr, respectively. Furthermore, a very weak diffraction spot of TiC corresponding lattice plane (200) in the SAD pattern of the Ti-Gr. It demonstrates that the TiC phase was generated in the Ti-0.5wt% Gr composite during SPS process at 900 °C. The NDs and TiC phase are existed in the Ti-NDs composite indicated from the results of the SAD pattern inserted in Figure 8(c). The high magnification TEM image in Figure 8(d) shows the lattice fringes of the NDs (0.206 nm).

It can be concluded that TiC phase is more easily formed in the Ti-NDs and Ti-Gr composites than in the Ti-MWCNTs composite. The generation of TiC phase during the SPS process at 900 °C, which can be demonstrated by the following equation related to the standard free energy ΔG of the second phase (TiC) formation [12, 23].

$$\Delta G = -184571.8+41.382T-5.042T\ln T+2.425\times 10\text{-}3T2-9.79\times 105/T(T<1939K) \qquad (1)$$

The ΔG for this reaction between Ti and C atoms at 1173K (900 °C) can be contained as - 175 kJ/mol, so it is apparent that in situ TiC phase via SPS technique at 900 °C was spontaneous creation. However, no TiC peaks observed in Ti-MWCNTs composites. It indicates that it is hard to occur a reaction in this composite, which can be attributed to their less activity. The MWCNTs have tubular structures are less active than the NDs and Gr.

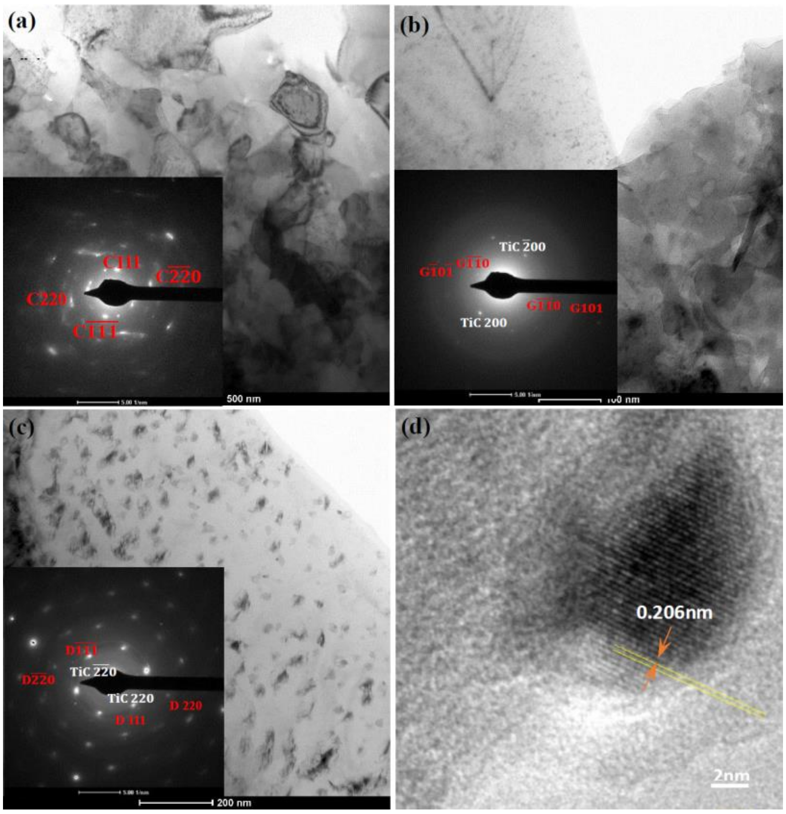

Figure 8: TEM micrographs of the Ti-0.5% MWCNTs/Gr/NDs nanocomposites with inserted SAD patterns (a, b, c) and HRTEM micrograph of a ND in the Ti matrix (d).

Consequently, dispersion strengthening of C reinforcements are regarded as the main strengthening mechanism in this work. On the other hand, as for Ti-NDs and Ti-Gr composite the solution strengthening also plays an important part in enhancing the mechanical properties. However, the single-layer Gr is easier to get agglomeration, and its layered structure is not benefit for a well bonding with the Ti matrix, which lead to a relative lower relative density. The nano-TiC phase generated in the sintering process can enhance the Ti matrix on account of the dispersion strengthening. It also can deteriorate the mechanical properties of the Ti with too much TiC in the samples. Due to the differences in thermal expansion coefficients between TiC and Ti matrix, the sites generated TiC phase tended to be the cracks origins, which worsen the mechanical properties. On the contrary, the long tubular structure of MWCNTs and the spherical structure of NDs are benefit to bond with the Ti matrix. Therefore, the well dispersion of the two kinds of nanocarbon reinforcements in the Ti matrix make a great contribution to achieve excellent mechanical properties of the composites. Depending on the well interface bonding between the tubular structured MWCNTs and the Ti matrix, the particles were difficult to be pulled out when fracture occurs under compression stress. Thus the Ti-0.5wt% MWCNTs composites has the best mechanical properties. In terms of a better mechanical properties of the Ti-NDs composites and nontoxicity of the NDs, the NDs particles provide a new promising reinforcement for their application in the biomedical field.

4 CONCLUSIONS

MWCNTs, Gr and NDs reinforced Ti matrix composites (TiMMCs) were prepared via SPS technique. The density of TiMMCs with 0.5wt% MWCNTs/NDs presented values up to 99.7%. Comparing to pure Ti, the mechanical properties of TiMMCs reinforced by nanocarbon are remarkably increased. The Ti-0.5wt% MWCNTs composite shows the best integrated mechanical properties which has the highest micro-hardness (28.6% higher than pure Ti) and fracture strength (σ_{bc}: 2193 MPa) at a few expense of ductility (ε: 62.95%). The layer structured Gr is not benefit for a well interface bonding with the Ti matrix with a relative lower density of the composites. The dispersion strengthening mechanism of MWCNTs, Gr and NDs play an important role in enhancing the mechanical properties of the Ti composites.

ACKNOWLEDGEMENTS

The authors gratefully acknowledge the financial supports from Natural Science Foundation of Jiangsu Province (No. BK20161419), Opening Project of State Key Laboratory of High Performance Ceramics and Superfine Microstructure at SICCAS (No.SKL201603SIC), Scientific Research Foundation for the Returned Overseas Chinese Scholars at State Education Ministry (No. 2015-1098), Jiangsu Key Laboratory for Advanced Metallic Materials (No. BM2007204), and the Fundamental Research Funds for the Central Universities (No. 2242017K40183).

REFERENCES

[1] Lütjering G, Williams JC, Gysler A. Titanium. In: Lütjering G, Williams JC, editor. Engineering Materials and Processes, vol 2, Heidelberg (Berlin, Germany): Springle, 2007, p. 379.

[2] Boyer R, Welsch G, Collings EW, editors. Materials properties handbook: titanium alloys. Ressell (Ohio, USA): ASM International in Metals Park (OH); 1994.

[3] Leyens C, Hausmann, Kumpfert J. Continuous fiber reinforced titanium matrix composites: fabrication, properties and applications. In: Leyens C, Peters M, editor. Titanium and titanium alloys, vol 12, Weinheim (Germany): Wiley-VCH Verlag GmbH & Co. KGaA, 2003; 305-330.

[4] Dion I, Baquey C, Monties JR, Havlik P. Haemocompatibility of TI6A14V alloy. Biomaterials, 1993; 14:122-6

[5] Ho WF, Chen WK, Wu SC, Hsu HC. Structure, mechanical properties, and grindability of dental Ti–Zr alloys. Journal of Materials Science: Materials in Medicine 2008; 19: 3179-86.

[6] Bogdanski D, Köller M, Müller D, Muhr G, Bram M, Buchkremer HP, Stöver D, Choi J, Matthias E. Easy assessment of the biocompatibility of Ni–Ti alloys by in vitro cell culture experiments on a functionally graded Ni–NiTi–Ti material. Biomaterials 2002; 23: 4549-55

[7] Okazaki Y, Gotoh E. Comparison of metal release from various metallic biomaterials in vitro. Biomaterials 2005; 26: 11–21.

[8] Vladimir A. Popov, Evgenij V. Shelekhov, Ekaterina V. Vershinina. Influence of reinforcing nonagglomerated nanodiamond particles on metal matrix nanocomposite structure stability in the course of heating. Eur J Inorg Chem 2016; 10:2122-2124.

[9] Hanada K, Yamamato K, Taguchi T, Osawa E, Inakuma M, Livramento V, et al. Further studies on copper nanocomposite with dispersed single-digit nanodiamond particles. Diamond Relat Mater 2007; 16(12): 2054–2057.

[10] Feng X, Sui JH, Feng Y, Cai W, Preparation and elevated temperature compressive properties of multi-walled carbon nanotube reinforced Ti composites. Mater Sci Eng A 2010; 527:1586-1589.

[11] Balandin A A, Ghosh S, Bao W, et al. Superior thermal conductivity of single-layer graphene [J]. Nano letters 2008; 8(3):902-907.

[12] Li SF, Sun B, Hisashi Imai, Takanori Mimoto, Katsuyoshi Kondoh. Powder metallurgy titanium metal matrix composites reinforced with carbon nanotubes and graphite. Compos A 2013; 48:57-66.

[13] R. Casati, M. Vedani. Metal matrix composites reinforced by nano-particles – a review. Metals 2014; 4 (1): 65–83.

[14] Dong SR, Tu JP, Zhang XB. An investigation of the sliding wear behaviour of Cu-matrix composite reinforced by carbon nanotube [J]. Material Science and Engineering A 2001; 313(2):83-87.
[15] Kondoh K, Threrujirapapong T, Imai H, Umeda J, Fugetsu B, Characteristics of powder metallurge pure titanium matrix composite reinforced with multiwall carbon nanotubes. Compos Sci Technol 2009; 69:1077-1081.
[16] Wang FC, Zhang ZH, Sun YJ, Liu Y, Hu ZY et al. Rapid and low temperature spark plasma sintering synthesis of novelcarbon nanotube reinforced titanium matrix composites. Carbon 2015; 95:396-407.
[17] M. Rashad, F.S. Pan, A.T. Tang, M. Asif, M. Aamir, Synergetic effect of graphene nanoplatelets (GNPs) and multi-walled carbon nanotube (MW-CNTs) on mechanical properties of pure magnesium, J. Alloy. Compd. 603 (2014) 111–118.
[18] F.Y. Chen, J.M. Ying, Y.F. Wang, S.Y. Du, Z.P. Liu, Q. Huang, Effects of graphene content on the microstructure and properties of copper matrix composites, Carbon 96 (2016) 836–842.
[19] Xiang Y, Zhang J, Jin C and Liu Y. Anti-friction properties of Cu10Sn-based composite containing nanometer diamond particles. Wear 2000; 242(1–2): 202–206.
[20] Melendez IM, Neubauer E, Angerer P, Danninger H, Torralba JM. Influence of nano-reinforcements on the mechanical properties and microstructure of titanium matrix composites. Compos Sci Technol 2011; 71:1154-1162.
[21] Fiorito S, Serafino A, Andreola F, Bernier P. Effects of fullerenes and single-wall carbon nanotubes on murine and human macrophages. Carbon 2006; 44:1100-1105.
[22] Combarros R G, Collado S, Diaz M. Toxicity of graphene oxide on growth and metabolism of pseudomonas putida. Journal of Hazardous Materials 2016; 310:246-252.
[23] Knacke, Kubaschewski O, Hesselmann K. Thermochemical properties of inorganic substance. Springer-Verlag, 1991; 264(2):2501-104.